Polymorphic Transformations in *sn*-1,3-Distearoyl-2-ricinoleyl-glycerol

Karima Boubekri[a,*], Junko Yano[b], Satoru Ueno[b], and Kiyotaka Sato[b]

[a]Venture Business Laboratory, Hiroshima University, Higashi-Hiroshima 739-8527, Japan, and [b]Faculty of Applied Biological Science, Hiroshima University, Higashi-Hiroshima 739-8528, Japan

ABSTRACT: Polymorphic transformations of *sn*-1,3-distearoyl-2-ricinoleyl-glycerol (SRS) have been studied with differential scanning calorimetry, X-ray powder diffraction (XRD), synchrotron radiation X-ray diffraction, and Fourier transform infrared spectroscopy (FTIR) techniques by using a 99.8% pure sample. Four polymorphs, α, γ, β'_2, and β'_1, were isolated. The thermal behavior of the four forms showed that the fusion of α at 25.8°C was followed by the crystallization of γ which melts at 40.6°C, and β'_2 and β'_1 revealed melting peaks at 44.3 and 48.0°C, respectively. No β form was observed, even when the two β′ forms were annealed around their melting points over one week. The XRD long spacing indicates that α packs into a double chain-length structure; however, γ and the two β′ phases pack into a triple chain-length structure. The polarized and nonpolarized FTIR spectra in methylene scissoring and methylene rocking regions indicated a parallel subcell packing in γ, and a mixture of orthorhombic perpendicular and parallel or hexagonal subcells in the β'_2 and β'_1 phases. Consequently, SRS exhibits quite a unique polymorphic behavior, compared to tristearoyl glycerol and *sn*-1,3-distearoyl-2-oleoyl-glycerol.

Paper no. J8970 in *JAOCS 76,* 949–955 (August 1999).

KEY WORDS: *sn*-1,3-Distearoyl-2-ricinoleyl-glycerol, DSC, FTIR, hydroxylated triacylglycerols, polymorphic transformations, synchrotron radiation X-ray diffraction, X-ray diffraction.

Triacylglycerols (TAG) are the major storage lipids in plants, especially in fruits, nuts, and seeds, and in the adipose tissue of more complex animals. The widespread nature and industrial importance of these compounds have led to a great interest in their composition and the physicochemical properties of their polymorphic modifications. Polymorphism is the ability to reveal different unit cell structures in crystal, originating from a variety of molecular conformations and molecular packing (1). Numerous studies on the polymorphism of a series of monoacid TAG, mixed saturated-acid TAG, and symmetric mixed saturated-unsaturated acid TAG have been carried out (2–4). Common to the nature of TAG polymorphism, α, β′, and β are the three typical forms in which α is least stable, β′ is metastable, and β is most stable. However, there are some exceptions which do not reveal the most stable β forms. For example, 1,2-palmitoyl-3-myristoyl-*sn*-glycerol (PPM) reveals three polymorphic transformations, α, β′, and the most stable, β'_1 (3). It seems that the molecular packing of TAG, influenced by the position of esterification on the glycerol backbone and the nature of the acyl chain, is most influential to the occurrence of the polymophic forms (4).

No information has been reported thus far on the polymorphism of triglycerides containing hydroxy fatty acids. *sn*-1,3-Distearoyl-2-ricinoleyl glycerol (SRS) is one of the saturated-unsaturated hydroxy acid triacylglycerols containing ricinoleic acid (12-hydroxy oleic acid), the major acid in castor oil (*Ricinus communis*). It has many industrial uses (5,6).

In this report, a systematic study of SRS has been conducted using a 99.8% pure sample. Particularly interesting were the effects of aliphatic chain-chain interactions involving hydroxy fatty acids on the polymophic structure.

MATERIALS AND METHODS

An SRS sample with a purity of 99.8% was prepared by Fuji Oil Co. Ltd. (Osaka, Japan), through enzymatic esterification using triricinoleyl and ethyl stearate. The occurrence of polymorphic modifications was examined by two modes of crystallization. The first one was a simple cooling of liquid from 70°C to varying temperatures of crystallization (T_c). The second crystallization was made by a melt-mediated transformation, in which more stable forms were crystallized after the melting of less stable forms by rapidly raising the temperature above their melting points.

Differential scanning calorimetry (DSC). A Rigaku Thermoplus DSC 8230 instrument (Tokyo, Japan) was used to increase the temperature range from −10 to 70°C at heating and cooling rates of 2, 5, and 10°C/min. The temperature of transformation was defined by computerized data-processing as a crossing point of a heating base line and the maximal slope of an initial endothermic line (onset temperature).

X-ray diffraction (XRD). Powder XRD patterns in SRS were examined using nickel-filtered CuKα radiation (λ = 0.1542 nm) to obtain short- and long-spacing values (Rigaku Geigerflex, Tokyo, Japan). Synchrotron radiation (SR)-XRD experiments were carried out at a beamline BL-15 A of the source which was operated at 2.5 GeV at the National Laboratory for High Energy Physics, Tsukuba, Japan.

*To whom correspondence should be addressed at Venture Business Laboratory, Hiroshima University, 2-313 Kagamiyama, Higashi-Hiroshima 739-8527, Japan. E-mail: boubekri@vbl.hiroshima-u.ac.jp

The double-focusing camera was operated at a wavelength of 0.15 nm for the SR-XRD. The details of the equipment cell employed in the SR-XRD study are described elsewhere (7). In brief, the X-ray scattering data were detected by position-sensitive proportional counters (PSPC) for the small-angle position. The distance between the sample and the PSPC was 1.28 m. The sample was placed in the center of a stainless steel sample cell with kapton film windows, which were sandwiched in a brass jacket. The temperature of the sample was controlled by thermostated water circulating between the sample cell and the brass jacket. A quick temperature jump was performed by utilizing two thermostated water baths connected by a magnetic switch. Temperatures of the sample were measured by thermocouples dipped in the sample. The thickness of the sample was 1 mm, and the SR-XRD spectra were taken at 10-s intervals.

Fourier transform infrared spectroscopy (FTIR). The powder sample was compressed detween two KBr windows, then melted to 60°C, and cooled to crystallize at varying temperatures. IR spectra were collected by using a Perkin-Elmer FTIR Spectrum 2000 spectrometer (Norwalk, CT) equipped with an *i*-series FTIR microscope. Two types of FTIR measurements were done: nonpolarized and polarized. The former type was applied to metastable polymorphs, and the polarized FTIR measurement was applied to the most stable forms. The polarization angle was varied from 0 to 180° in 25° increments.

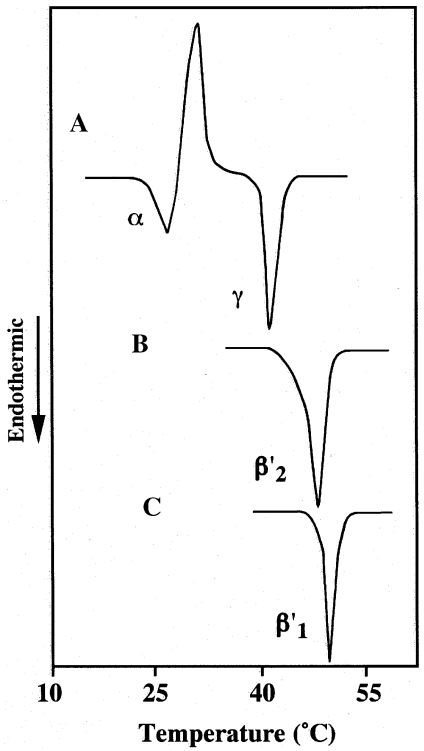

FIG. 1. Differential scanning calorimetry heating thermograms of the polymorphs of *sn*-1,3-distearoyl-2-ricinoleyl-glycerol (SRS) at a heating rate of 10°C/min. In (A), the $\alpha \rightarrow \gamma$ transformation, α was crystallized at –6°C; (B) β'_2 was obtained from γ-melt mediation at 41°C; (C) β'_1 was obtained after incubating the β'_2 phase at 44°C for 10 h.

RESULTS

Figure 1 shows the DSC melting thermograms of SRS taken at a heating rate of 10°C/min. Four polymorphic transformations were obtained. The fusion of α at 25.8°C was soon followed by the crystallization of γ with a melting point of 40.6°C. The melting points of the two β' forms, β'_2 and β'_1, were 44.3 and 48.0°C, respectively.

The XRD short-spacing and long-spacing patterns are shown in Figure 2 and Table 1. α has a single peak at 4.19 Å. γ has two strong peaks at 4.72 and 3.93 Å, and two weak peaks at 4.40 and 3.64 Å. β'_2 has two strong peaks at 4.25 and 4.00 Å, whereas different strong peaks were observed for β'_1.

The long-spacing values, which reflect the lamella thickness of each polymorph, are shown in Figure 2 and Table 1. α is considered a double chain length and the other three forms as triple chain length structures.

We examined the polymorphic crystallization using the SR-XRD. It should be noted that the spectra were taken at 10-s intervals. Figure 3 shows the γ-melt and β'_2-melt-mediated crystallizations, in which a stepped temperature variation induced the transformation of γ melt $\rightarrow \beta'_2$ melt $\rightarrow \beta'_1$. The γ form was crystallized at 26°C, showing the small-angle reflections of 71 (001 reflection) and 35.5 Å (002 reflections) which gave a long-spacing value of 71 Å. About 2 min after the temperature jump from 26 to 41°C, the β'_2 form started to crystallize as revealed by the diffraction peak of 69.7 Å (002 reflection). About 10 min after the temperature jump to 45°C, the long-spacing spectrum of 68.5 Å for β'_1 appeared and increased in intensity, revealing the crystallization of the β'_1 form. Figure 3 demonstrates the existence of two β' forms with different melting points and long-spacing values.

In order to analyze the subcell structures and molecular conformations of acyl chains of SRS, two types of FTIR measurements were carried out: nonpolarized for α and γ forms, and polarized measurements for the two β' forms. Figure 4 shows the FTIR spectra in polymethylene scissoring $\delta(CH_2)$ and rocking $r(CH_2)$ regions of α, γ, β'_2, and β'_1. A single band was detectable in α at 1467 cm^{-1} in the $\delta(CH_2)$ regions, and at 721 cm^{-1} in the $r(CH_2)$ regions. The two spectral bands indicated the presence of hexagonal subcell packing in the α form. Furthermore, in the γ form, a single band is present at 1471 and 717 cm^{-1}, reflecting the presence of parallel subcell packing (8).

The polarized spectra of β'_2 and β'_1 were rather complicated. At least two components of $\delta(CH_2)$ modes were observed at 1466 and 1470 cm^{-1}, and at 720 and 726 cm^{-1} of the $r(CH_2)$ modes. In the polarized spectra, the peak at 726 cm^{-1} became strongest at the polarization angle of 90°, where the intensity of 720 cm^{-1} became weak. The same property was observed in the two components of scissoring modes, reflecting the $O_\perp$ subcell packing (9). The complexity in the polarization properties of these two components was not clarified, in contrast to those of the typical $O_\perp$ subcell structure which was observed in β'_1 of ppm (10).

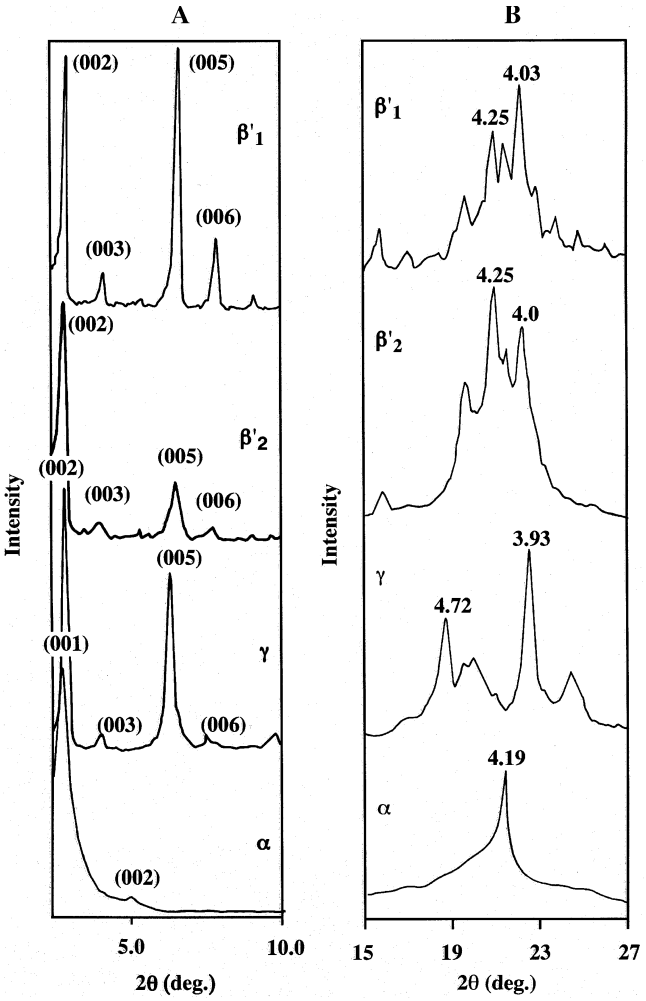

FIG. 2. X-ray diffraction long-spacing (A), and short-spacing (B) spectra of four polymorphs of SRS. See Figure 1 for abbreviation.

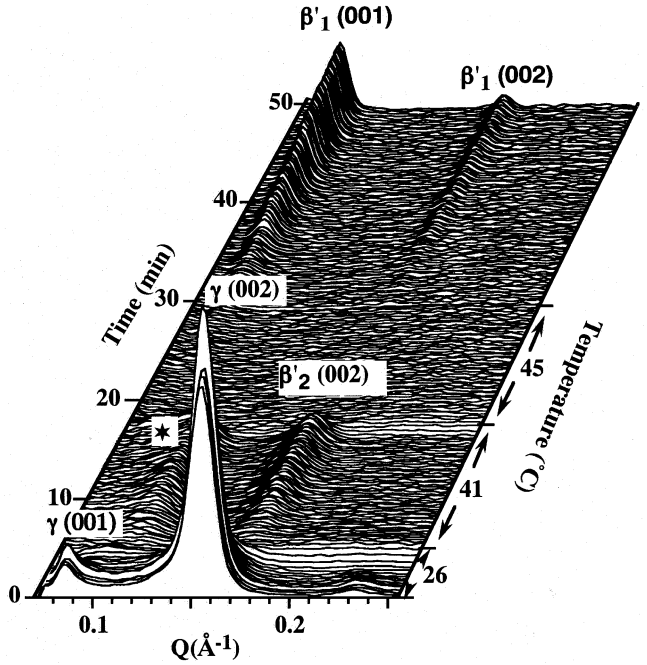

FIG. 3. Synchrotron radiation X-ray diffraction spectra of the γ-melt mediated crystallization of SRS. The heating steps were 9.5°C/min without annealing. ✶, unknown polymorph. See Figure 1 for abbreviation.

Figure 5 shows the FTIR spectra of the γ, β'_2, and β'_1 of SRS, compared to the β form of tristearin (SSS) in the methylene-wagging progression bands region of 1500 to 1100 cm^{-1} as shown in Table 2 (11). The bands marked with open circles are of the all-*trans* stearoyl chains at the *sn*-1 and -2 positions, and those with wedges are the bent stearoyl chain at the *sn*-3 position. The peak positions in the γ and β'_2 forms are similar to the peak positions in the β form of SSS. However, the spectra of the β'_1 form revealed two additional peaks at 1226.5 and 1242.5 cm^{-1}.

DISCUSSION

The present work is the first investigation of the polymorphic transformations in SRS. Four polymorphs, α, γ, β'_2, and β'_1 were identified by unique melting points examined by DSC and XRD short- and long-spacing spectra. As to the absence of the β form, which was revealed in many TAG as the most stable form, a careful study was conducted with two types of crystallization: thermal annealing of β'_1 just below its melting temperature (46°C) over 1 wk, and solvent crystallization in acetonitrile solution saturated with respect to β'_1 over 1 wk. The former process may accelerate the solid-state transformation from β'_1 to more stable forms, if any. The latter process also induces the crystallization of the most stable forms, as revealed in the β forms of SOS (12,13). However, no occurrence was detectable in the two experiments for SRS. Thus, one may conclude that there is no β form in SRS.

It is quite interesting to compare the physical properties of the SRS polymorphs with those of SSS (15,16) and SOS (12–14). Polymorphic forms, melting temperatures and en-

TABLE 1
X-ray Diffraction Long-Spacing and Short-Spacing of Polymorphs of SRS[a]

Polymorph	Long-spacing (Å)	Short-spacing (Å)
α	48.7	4.19(vs)
γ	71.0	4.72(s), 4.52(w), 4.4 (w), 3.93(vs), 3.63(w)
β'_2	69.71	5.64(w), 4.54(m), 4.25(vs), 4.13(w), 4.0 (s)
β'_1	68.54	5.64(w), 4.53(w), 4.25(s), 4.13(m), 4.03(vs), 3.9(w), 3.74(w)

[a]SRS, *sn*-1,3-distearoyl-2-ricinoleyl-glycerol; vs, very sharp; s, sharp; w, weak; m, medium.

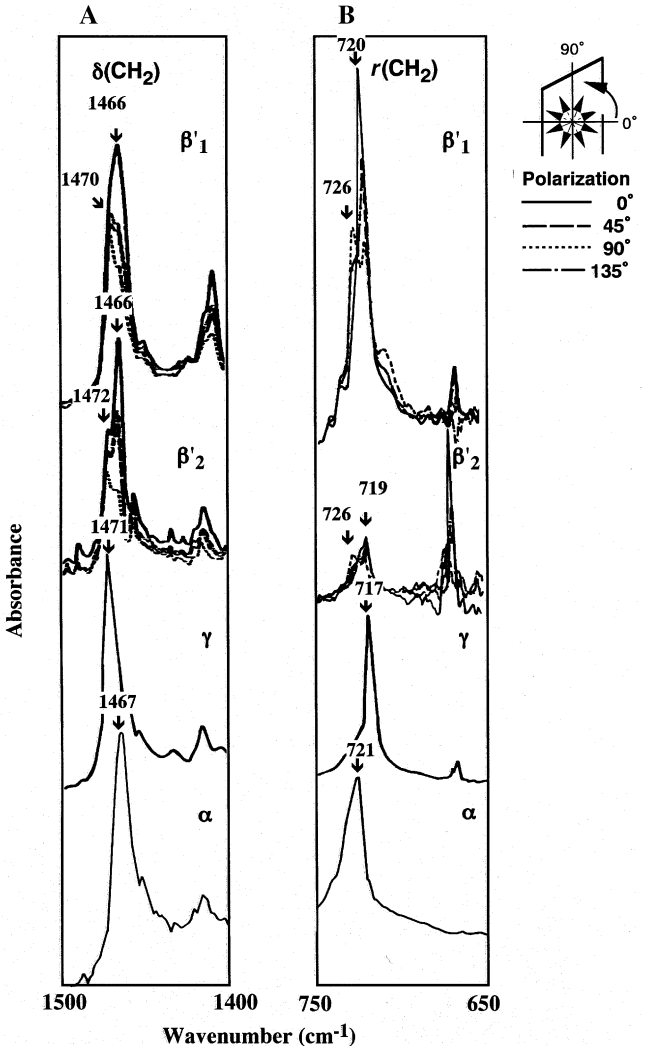

FIG. 4. Fourier transform infrared spectroscopy (FTIR) spectra of SRS, (A) in CH_2 scissoring, and (B) in CH_2 rocking regions. See Figure 1 for other abbreviation.

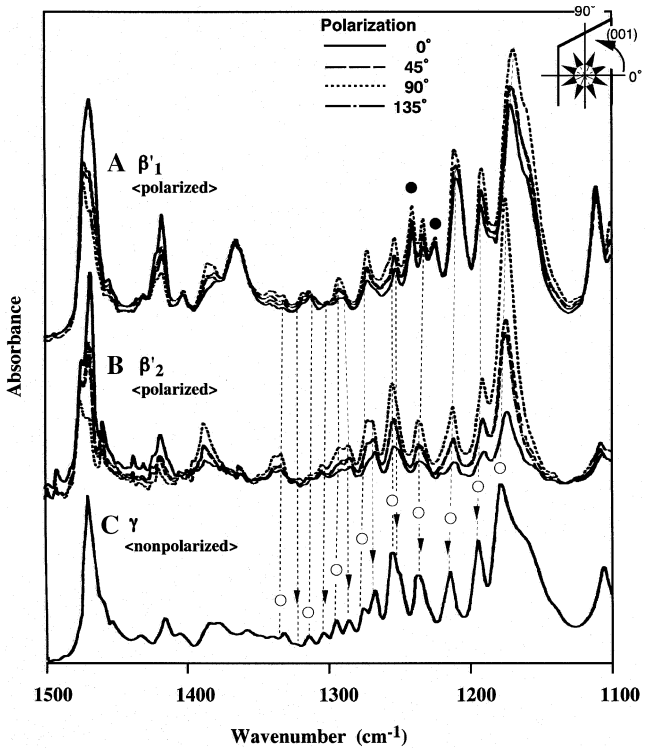

FIG. 5. FTIR spectra in the region of 1500–1100 cm^{-1}. In (A), polarized spectra of β'_1, (B) polarized spectra of β'_2, and (C) nonpolarized spectrum of γ of SRS. ○, *Trans* stearoyl chains at the *sn*-1 and -2 position; ▼, the bent stearoyl chains at the *sn*-3 position, as shown in Table 2 (11); ●, additional peaks. See Figures 1 and 4 for abbreviations.

thalpies of fusion and entropy are summarized in Table 3. The thermodynamic values of the α forms of the three TAG decreased in a sequence of SSS, SRS, and SOS. This can be interpreted in terms of the steric hindrances between the stearoyl, ricinoleyl (SRS), and oleoyl (SOS) chains, in the double chain-length structure. As for SRS and SOS, with acids differing by only one OH group, the thermodynamic values of SRS are higher than those of SOS. It is interesting to see, as an example, that the ΔH value of the β'_1 phase of SRS is greater than that of the β′ form of SOS by 80 kJ/mol, and even of the most stable β_1 form of SOS by 34 kJ/mol. As for ΔS values between SRS and SOS, the differences in ΔS (J/mol·K) were 237 between SRS β'_1 and SOS β′, and 98 between SRS β'_1 and SOS β_1. The same comparison can be made between the β'_2 form of SRS and the two forms of SOS. From these data, it can be suggested that the stability and ordered conformation of the β'_2 and β'_1 forms of SRS are due to the presence of hydrogen bonds in the OH groups of ricinoleic acid moiety.

TABLE 2
Frequencies and Assignments of Methylene-Wagging Progression Bands of Tristearoylglycerol Form

SSS[a]	
Band position (cm^{-1})	Assignment[b]
1182	W1-t
1195	W2-t, W1-g
1214	W2-g
1215	W3-t
1234	W3-g
1236	W4-t
1256	W5-t, W4-g
1271	W5-g
1275	W6-t
1287	W6-g
1292	W7-t
1305	W7-g
1316	W8-t
1322	W8-g
1332	W9-t
1339	W9-g
1347	W10-t
1352	W10-g
1359	W11-t

[a]SSS, tristearoyl glycerol. The IR bands as per Yano *et al.* (11).
[b]W, wagging progression band (ν_3 mode); t, straight *sn*-1,2 chains; g, bent *sn*-3 chain.

TABLE 3
Thermal Data of SRS, SSS and SOS Polymorphs

	Polymorph	mp (°C)	ΔH (kJ/mol)	ΔS (J/mol·K)
SRS	α	25.8	58.1[a]	194.35
	γ	40.6	119.64	381.32
	β'_2	44.3	171.19	539.29
	β'_1	48.0	184.76	575.31
SSS[b]	α	55.0	109.3	333.08
	β′	61.64	142.8	426.54
	β	73.0	188.4	544.27
SOS[c]	α	23.5	47.7	160.79
	γ	35.4	98.5	319.23
	β′	36.5	104.8	338.47
	β_2	41.0	143.0	455.19
	β_1	43.0	151.0	477.62

[a]Enthalpy of crystallization was measured on α.
[b]Data from References 15 and 16.
[c]Data from Reference 12. SOS, *sn*-1,3-distearoyl-2-oleoyl-glycerol; see Tables 1 and 2 for other abbreviations.

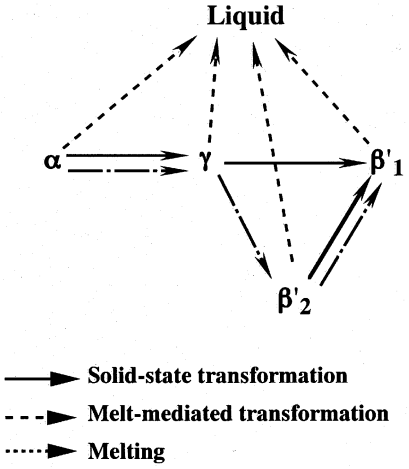

FIG. 6. The polymorphic transformations in SRS. See Figure 1 for abbreviation.

The occurrence of β′ forms has been reported in the monoacid (17,18) and mixed-acid TAG (10). In several palmitoelaidic triglycerides, three polymorphic forms, α, β'_2, and β'_1, have been reported (19), where all polymorphs crystallized in the double chain-length packing. As for SRS, the two β′ forms reveal a distinct difference. There is a difference in the melting point of about 4°C and small additional short-spacing peaks appear, particularly in β'_1 form.

It is assumed that the two β′ forms may reveal the mixture of two types of subcell structures, $O_\perp$ because of the appearance of the two peaks of scissoring and rocking bands (Fig. 4), and the other may be parallel or hexagonal packing due to the higher intensity at 720 cm^{-1} (20).

For the clarification of the subcell structures of the β′ forms of SRS, there are some indications concerning the different molecular structures of ricinoleyl chains as revealed by the methylene progression bands in the FTIR spectra (Fig. 5). The two stearoyl chains of SRS in the three polymorphic forms (γ, β'_2, β'_1) assume the same conformations as in β of SSS. However, β'_1 of SRS has two additional peaks which are not from the stearoyl chains, but from ricinoleyl chains. These reflect the ordered molecular conformation in the ricinoleic acyl chain.

The melt-mediated and solid-state transformations of SRS examined by DSC and SR-XRD are schematically summarized in Figure 6. The α-melt mediation induced the occurrence of γ, β'_2, and β'_1 forms successively. Table 4 summarizes the solid-state transformation rates. α directly transformed from the double chain-length structure to γ of the triple chain-length structure, which transformed into the most stable β'_1 form by holding the temperature at 38°C for 9 h. The $\beta'_2 \rightarrow \beta'_1$ transformation occurred over 12 h at 38°C.

Figure 7 illustrates the structural models of the four polymorphs of SRS. In the α form of the double chain-length structure, both the stearoyl and ricinoleyl chains are in a disordered packing state, showing the hexagonal subcell. As a result, the possibility for the OH groups to make chemical bonds is weak. In the γ and the two β′ forms, chain sorting gave rise to the separation of the stearoyl and ricinoleyl chains to form the triple chain-length structure. The subcell structures are probably of parallel type in γ and $O_\perp$, and possibly of parallel or hexagonal type in β'_2 and β'_1 polymorphs. The $O_\perp$ subcell structure raised from the stearoyl leaflet as revealed in β′ of SOS (14). In the triple-chain structures the possibility of OH groups to make chemical bonds is high.

TABLE 4
Rate of Polymorphic Transformations of SRS in Solid State[a]

	α→γ	γ→β'_1	$\beta'_2 \rightarrow \beta'_1$
SRS	8 h, at 18°C	9 h, at 38°C	12 h, at 38°C

[a]See Table 1 for abbreviation.

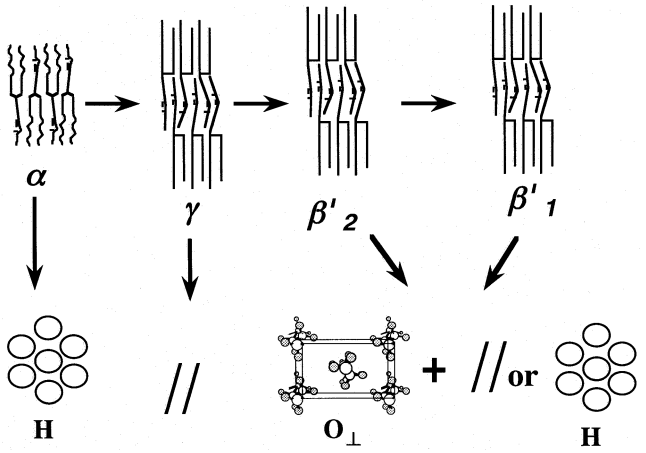

FIG. 7. Structure models of polymorphs in SRS, with respect to specific subcell structures. See Figure 1 for abbreviation.

Figure 8 illustrates two possible models of the molecular features of the acyl chain arrangements and the subcell structures of the ricinoleic acid leaflets in the β'_1 form, assuming that the steric acid leaflets are packed in the $O_\perp$ subcell. The two models are based on two different types of stabilization: hydrogen bonding and *cis*-double bond/methyl end packing.

In model A, the hydrogen bondings at the hydroxyl groups are stabilized since they are formed between the nearest neighboring molecules, side by side. In order to avoid the steric hindrance between the hydrogen bonding and the C–H bond at the twelfth hydrocarbon atom, the triclinic parallel-type subcell is most favored. All the hydrogen-bonding chains in a repeating lamella are placed on the single plane normal to the chain axis of the aliphatic chains. The steric hindrance, however, of the *cis*-double bond conformations and the methyl end packing are not stabilized. This structure forms vacancies at the terminal end of the ricinoleic chains, giving rise to elongated lamella distance, equivalent to six excess carbons, *ca*. 7.5 Å. In fact, the long spacing values of γ (71.0 Å), β'_2 (69.71 Å), and β'_1 (68.54 Å) do not make this model plausible.

In addition, the unstabilized methyl end packing may decrease the ΔH and ΔS values for fusion in SRS, compared to SOS. However, the two values of SRS are much higher than those of SOS (Table 3).

By contrast, model B assumes that the *cis*-double bonds are arranged between the nearest neighboring molecules side by side, so that the steric hindrance due to the *cis*-olefinic conformation and the methyl end packing of the ricinoleic chains is minimized. As to the hydrogen bonding, all the hydrogen-bonding chains in a repeating lamella are not placed on the single plane. The orthorhombic parallel-type subcell is favored to avoid the steric hindrance between the hydrogen-bonding chains and the neighboring zig-zag hydrocarbon chains, taking a superstructure-type subcell with the subcell (a_s) axis whose dimensions are twice as long as the corresponding subcell axis in model A.

Model B may justify the observed long spacing and the ΔH and ΔS values of the β'_1 form. Furthermore, one may assume that the stabilization of the orthorhombic-type subcell of the ricinoleic acid leaflets, due to the hydrogen bond formation, may also cause the stabilization of the $O_\perp$ subcell in the stearic acid leaflets, eventually leading to the β′ form becoming the most stable polymorph in SRS. Further clarification is needed to resolve this molecular feature.

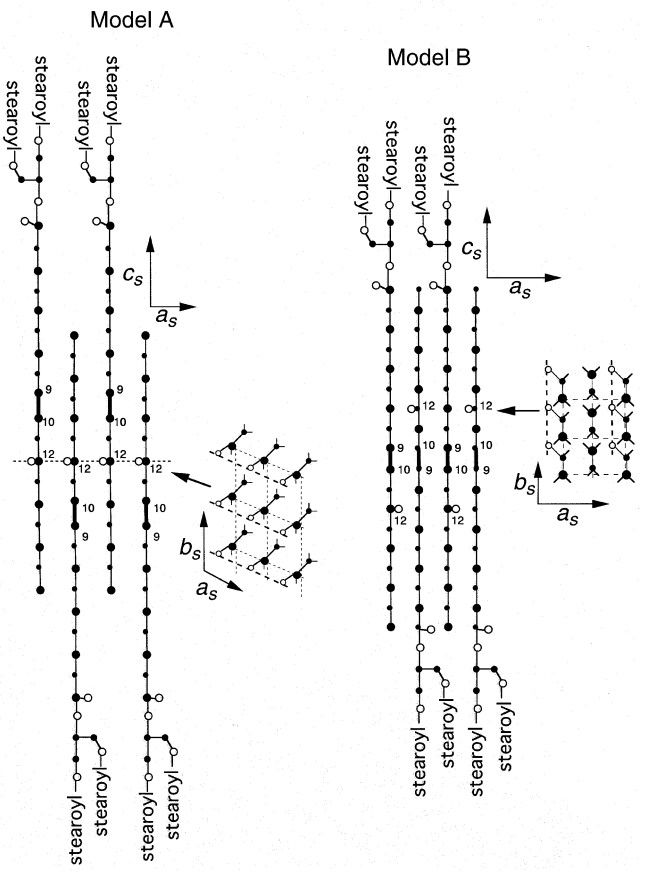

FIG. 8. Molecular features of hydrogen bonding (dotted lines) and subcell structures (a_s, b_s, and c_s subcell parameters) of ricinoleic acid leaflets in β′ forms of SRS. ○, oxygen atoms and ●, carbon atoms, in which large and small circles are placed at upper and lower positions in the zig-zag hydrocarbon planes, respectively.

ACKNOWLEDGMENTS

The authors are indebted to Venture Business Laboratory, Hiroshima University, for financial support and to Nobuo Sagi of the Fuji Oil Company, Tsukuba, for supplying the sample.

REFERENCES

1. Larsson, K., Molecular Arrangement in Glycerides, *Fette Seifen Anstrichm. 74*:136–143 (1972).
2. Garti, N., and K. Sato, *Crystallization and Polymorphism of Fats and Fatty Acids, Surfactant Science Series*, Marcel Dekker Inc., New York, 1988, Vol. 31, pp. 9–95.
3. Kodali, D.R., D. Atkinson, and D.M. Small, Polymorphic Behavior of 1,2-Dipalmitoyl-3-lauroyl (PP12)- and 3 Myristoyl (PP14)-*sn*-Glycerols, *J. Am. Oil Chem. Soc. 31*:1853–1864 (1990).
4. Sato, K., Polymorphism of Pure Triacylglycerols and Natural Fats, in *Advances in Applied Lipid Research*, edited by F. Padley, JAI Press Inc., London, 1996, Vol. 2, pp. 213–268.
5. Gaginella, T.S., and S.F. Phillips, Current View of an Ancient Oil, *Dig. Dis. 20*:1171–1177 (1975).
6. Orthoefer, F.T., Vegetable Oils, in *Bailey's Industrial Oil and Fat Products,* edited by Y.H. Hui, John Wiley & Sons, Inc., New York, 1996, Vol. 1, pp. 19–43.
7. Ueno, S., A. Minato, H. Seto, Y. Amemiya, and K. Sato, Synchrotron Radiation X-Ray Diffraction Study of Liquid Crystal Formation and Polymorphic Crystallization of SOS (*sn*-1,3-distearoyl-2-oleoyl glycerol), *J. Phys. Chem. 101*:6847–6854 (1997).
8. Abrahamsson, S., B. Dahlen, H. Lofgren, and I. Pascher, Lateral Packing of Hydrocarbon Chains, *Prog. Chem. Fats Other Lipids 16*:125 (1978).
9. Chapman, D., X-Ray Diffraction Studies, in *The Structure of Lipids by Spectroscopic and X-Ray Techniques*, edited by D. Chapman, Wiley & Sons, New York, 1965, pp. 221–315.
10. Yano, J., F. Kaneko, M. Kobayashi, D.R. Kodali, D.M. Small, and K. Sato, Structural Analysis and Triacylglycerols Poly-

morphs with FTIR Techniques. 2. β'_1-Form and 1,2-Dipalmitoyl-3-myristoyl-*sn*-glycerol, *J. Phys. Chem. 101*:8120–8128 (1997).
11. Yano, J., F. Kaneko, M. Kobayashi, and K. Sato, Structural Analysis and Triacylglycerols Polymorphs with FTIR Techniques. 1. Assignments of CH_2 Progression Bands of Saturated Monoacid Triglycerols, *Ibid. 101*:8112–8119 (1997).
12. Sato, K., T. Arishima, Z.H. Wang, K. Ojima, N. Sagi, and H. Mori, Polymorphism of POP and SOS. I. Occurrence and Polymorphic Transformation, *J. Am. Oil Chem. Soc. 66*:664–674 (1989).
13. Arishima, T., N. Sagi, H. Mori, and K. Sato, Polymorphism of POS. I. Occurrence and Polymorphic Transformation, *Ibid. 68*:710–715 (1991).
14. Yano, J., S. Ueno, K. Sato, T. Arishima, N. Sagi, F. Kaneko, and M. Kobayashi, FTIR Study of Polymorphic Transformations in SOS, POP, and POS, *J. Phys. Chem. 97*:12967–12973 (1993).
15. Ollivon, M., and R. Perron, Measurements of Enthalpies and Entropies of Unstable Crystalline Forms of Saturated Even Monoacid Triglycerides, *Thermochim. Acta 53*:183–194 (1982).
16. Hagemann, J.W., and J.A. Rothfus, Polymorphism and Transformation Energetics of Saturated Monoacid Triglycerides from Differential Scanning Calorimetry and Theoretical Modeling, *J. Am. Oil Chem. Soc. 60*:1123–1131 (1983).
17. Bociek, S.M., S. Ablett, and I.T. Norton, ^{13}C-HMR Study of the Crystal Polymorphism and Internal Mobilities of the Triglycerides, Tripalmitin and Tristearin, *Ibid. 62*:1261–1266 (1985).
18. Eads, T.M., A.E. Blaurock, R.G. Bryant, D.J. Roy, and W.R. Croasmun, Molecular Motion and Transitions in Solid Tripalmitin Measured by Deuterium Nuclear Magnetic Resonance, *Ibid. 69*:1057–1068 (1992).
19. Elizabettini, P., G. Lognay, A. Desmedt, C. Culot, N. Istasse, E. Deffense, and F. Durant, Synthesis and Physicochemical Characterization of Mixed Diacid Triglycerides That Contain Elaidic Acid, *Ibid. 75*:285–291 (1998).
20. Suzuki, M., T. Ogaki, and K. Sato, Crystallization and Transformation of α, β, and γ Polymorphs of Ultra-Pure Oleic Acid, *Ibid. 62*:1600–1604 (1985).

[Received August 10, 1998; accepted May 3, 1999]